Published in final edited form as:
Genomics. 2009 September ; 94(3): 188–195. doi:10.1016/j.ygeno.2009.05.011.

Candidate Agtr2 influenced genes and pathways identified by expression profiling in the developing brain of *Agtr2*$^{-/y}$ mice

Traci L. Pawlowski[a,b,d], **Silvia Heringer-Walther**[c,e], **Chun-Huai Cheng**[b], **John G. Archie**[a,f], **Chin-Fu Chen**[b], **Thomas Walther**[c,g], and **Anand K. Srivastava**[a,b,*]

[a]J. C. Self Research Institute of Human Genetics, Greenwood Genetic Center, Greenwood, South Carolina

[b]Department of Genetics and Biochemistry, Clemson University, Clemson, South Carolina

[c]Department of Cardiology, Charité, Campus Benjamin Franklin, Berlin, Germany

Abstract

Intellectual disability (ID) is a common developmental disability observed in one to three percent of the human population. A possible role for the Angiotensin II type 2 receptor (AGTR2) in brain function, affecting learning, memory, and behavior, has been suggested in humans and rodents. Mice lacking the *Agtr2* gene (*Agtr2*$^{-/y}$) showed significant impairment in their spatial memory and exhibited abnormal dendritic spine morphology. To identify *Agtr2* influenced genes and pathways, we performed whole genome microarray analysis on RNA isolated from brains of *Agtr2*$^{-/y}$ and control male mice at embryonic day 15 (E15) and postnatal day one (P1). The gene expression profiles of the *Agtr2*$^{-/y}$ brain samples were significantly different when compared to profiles of the age-matched control brains. We identified 62 differently expressed genes ($p \leq 0.005$) at E15 and in P1 brains of the *Agtr2*$^{-/y}$ mice. We verified the differential expression of several of these genes in brain samples using quantitative RT-PCR. Differentially expressed genes encode molecules involved in multiple cellular processes including microtubule functions associated with dendritic spine morphology. This study provides insight into *Agtr2* influenced candidate genes and suggests that expression dysregulation of these genes may modulate *Agtr2* actions in the brain that influences learning and memory.

Keywords

Learning and memory; Intellectual Disability; Dendritic spine; Expression profiling; Agtr2

Introduction

Intellectual disability (ID), also known as mental retardation, is a genetically and clinically heterogeneous condition characterized by below average intellectual functioning (IQ<70) in

*Correspondence author. J.C. Self Research Institute of Human Genetics, Greenwood Genetic Center, 113 Gregor Mendel Circle, Greenwood, SC 29646, USA. Tel. 1 864 388 1806; Fax: 1 864 388 1808; E-mail: anand@ggc.org (A.K. Srivastava).
[d]Present address: Neurogenomics Division, TGEN, Phoenix, Arizona;
[e]Present address: Department of Obstetrics, University of Leipzig, Leipzig, Germany;
[f]Present address: Department of Biomolecular Engineering, University of California at Santa Cruz, Santa Cruz, California;
[g]Present address: Department of Biomedical Sciences, Hull York Medical School, University of Hull, UK.

conjunction with significant limitations in adaptive functioning. The genetic component of ID likely includes deficiencies in the function of a large number of genes distributed throughout the human genome [1].

Angiotensin II (Ang II), a component of the renin-angiotensin system (RAS), mediates its majority of functions through two major Ang II receptor subtypes, type 1 receptor (AGTR1) and type 2 receptor (AGTR2). Studies in mice and humans indicated a possible role for AGTR2 in learning, memory, and behavior [2–6]. Neurological findings in *Agtr2*-deficient male mice (*Agtr2*$^{-/y}$) provided an initial hypothesis of a likely role for Agtr2 in the brain [7,8]. Recently, a detailed examination of the *Agtr2*-deficient mice revealed significant impairment in their learning performance in a spatial memory task [9]. These mice exhibited abnormal dendritic spine morphology [9], a feature previously shown to be associated with several cases of ID [10–12].

AGTR2 is a 323-residue G-protein-coupled receptor transcribed from an X-linked gene. Expression of the *Agtr2 gene* has been shown to be transiently expressed in the mesenchyme of the rat fetus, in various brain structures through embryonic development, with its expression declining rapidly after birth and becoming restricted to a few organs including the brain [13]. At the cellular level, Agtr2 has been shown to be localized in neurons [14]. Involvement of Agtr2 in several signaling cascades influencing neurite outgrowth and elongation, neuronal differentiation, cell proliferation, growth inhibition and induction of apoptosis has emerged in recent years but none is fully defined. Several proteins, avian erythroblastosis oncogene B 3 receptor (ERBB3), zinc finger and BTB domain containing 16 (ZBTB16), solute carrier family 9 (sodium/hydrogen exchanger), member 6 (NHE6/SLC9A6), and mitochondrial tumor suppressor 1 (MTUS1), have been found to interact with regions of AGTR2 [15–18]. Interestingly, defects in the NHE6/SLC9A6 gene have recently been found to cause Christianson syndrome, an X-linked ID condition [19].

To assess the impact of *Agtr2* on gene expression and to identify dysregulated genes and pathways relevant to Agtr2 function, we profiled gene expression patterns of *Agtr2*$^{-/y}$ brains at developmental stage E15 and at birth and compared them to profiles of the age matched control brains. This study revealed a number of candidate genes and cellular processes that may potentially influence brain structure and function critical for learning and memory.

Results

Microarray analysis

Expression microarray analysis was performed using RNA isolated from brains of male Agtr2-deficient (*Agtr2*$^{-/y}$) and control mice of identical genetic background using Agilent whole mouse genome 44K expression arrays. Gene expression profiles of the *Agtr2*$^{-/y}$ brain samples were compared to profiles of the control brains for two developmental stages, E15 and birth (P1). Multiple biological replicates (eight *Agtr2*$^{-/y}$ and six control brains at E15 and four *Agtr2*$^{-/y}$ and four control brains at birth) were analyzed individually using a dye swap experimental design. The raw data were analyzed as detailed in the Materials and methods. Hierarchical clustering of each developmental set demonstrated that, overall, the *Agtr2*$^{-/y}$ mouse brains had significantly different expression patterns than controls (Fig. 1).

Data analysis revealed 62 differently expressed genes (52 up-regulated and 10 down-regulated, $p \leq 0.005$) (Table 1). A similar analysis in P1 brains resulted in a list of 50 up-regulated and 12 down-regulated genes (Table 2) identified with a fold change greater than or equal to 1.4 and p-value less than 0.005. Fold change was computed with Bioconductor limma software with a log2 transformation. Two genes, phosphatidylserine decarboxylase

(*Pisd*) and RAB30, member RAS oncogene family (*Rab30*), were found to be upregulated at both developmental stages (Tables 1 and 2).

We further validated the differential expression of a subset of genes identified by microarray analysis using an independent method. We performed quantitative real-time PCR analysis of transcripts randomly selected from the E15 list (Table 1) and P1 list (Table 2). Changes in expression of these genes in *Agtr2*$^{-/y}$ brain samples relative to control brains were in agreement with the direction of the expression profile array data (Table 3). Four genes tested were significantly ($p \leq 0.05$) differentially expressed by qRT-PCR. The expression of seven other genes were comparatively not statistically significant ($p \geq 0.07$) but reflected the direction and approximate magnitude of fold-change as observed on the expression arrays. Failure to reach statistical significance in these cases may be either due to some potential false positive findings in the expression array data or due to the small sample size (four controls and four knockouts) used for the secondary verification by qRT-PCR.

Functional grouping

In an attempt to uncover common functions among the dysregulated genes, we classified genes into gene ontology groups. A summary of functions for dysregulated genes in the E15 knockouts are presented in Supplementary Table 1. The largest gene categories over-expressed in E15 *Agtr2*$^{-/y}$ brains are transcription factors and genes with Agtr1-related functions (Supplementary Table 1). Other categories include genes involved in microtubule and actin processing, cell adhesion, protein transport and/or binding, nucleic acid binding, immunity, cell cycle arrest, and ubiquitin/proteosome function. In the E15 *Agtr2*$^{-/y}$ brains, genes predominantly involved in apoptosis, polo-like kinase 1 (*Plk1*), prostaglandin E synthase 2 (*Ptges2*), growth factor erv1 (*Gfer*) and ubiquitin-conjugating enzyme E2M (*Ube2m*), were down-regulated.

Up-regulated genes in the P1 *Agtr2*$^{-/y}$ brains were involved in protein binding and transport, RNA processing, DNA binding, transcription, glutamate metabolism, cell adhesion as well as cytoskeleton and microtubule expression. A complete summary of the categories is listed in Supplementary Table 2.

Examination of the P1 down-regulated results (Supplementary Table 2) show that some of the gene functions involved are histone modification (*Nasp*, nuclear autoantigenic sperm protein and *Ppp2cb*, protein phosphatase 2 (formerly 2A), catalytic subunit, beta isoform), nucleotide metabolism (*Itpa*, inosine triphosphatase), NADP+ activity (*Idh1*, isocitrate dehydrogenase 1 (NADP+) soluble), protein ubiquitination (*Fbxo11*, F-box protein 11 and *Ndfip2*, Nedd4 family interacting protein 2), rRNA processing (*Frg1*, FSHD region gene 1), chromatin remodeling (*Chmp5*, chromatin modifying protein 5), and calcium ion binding (*Creld1*, calcium ion binding, cysteine-rich with EGF-like domains 1).

Pathway and network analysis

Pathway Studio (Ariadne, Rockville, MD) was used to visualize common functions for dysregulated genes in the E15 *Agtr2*$^{-/y}$ brains. Examining the up-regulated genes in the *Agtr2*$^{-/y}$ E15 brains with 1.3 fold or greater expression revealed a complex picture. Among the up-regulated genes, microtubule-associated protein 2 (*Mtap2*), microtubule-associated protein 1B (*Mtap1B*), A kinase (PRKA) anchor protein (*Akap9*), formin binding protein 1-like (*Fnbp1l*), triple functional domain (*Trio*) and Src-like-adaptor 2 (*Sla2*) are all associated with microtubule, actin and cytoskeleton function (Fig. 2A). Agtr2 has previously been shown to down-regulate MAP1B (Mtap1b) but up-regulate MAP2 (Mtap2) in PC12W cells [20]. In this study, Mtap2 and Mtap1b are both up-regulated in the E15 *Agtr2*$^{-/y}$ brains. MAP2 has previously been shown to be phosphorylated by JNK and subsequently defines

dendritic shape in the brain [21]. MAP2 is found in dendrites and is crucial for microtubule stability [22]. Mtap1b is found in growth cones and is needed for neurite outgrowth [20]. These genes also regulate actin along with *Fnbp1l* and *Sla2 genes* [23] which are up-regulated in E15 *Agtr2*$^{-/y}$ brain. Genes involved in regulation of microtubules, adducin 1 (alpha) (*Add1)*, echinoderm microtubule associated protein like 5 *(Eml5)*, Huntingtin (*Htt*), hook homolog 1*(Hook1)*, NudC domain containing 3 (*Nudcd3)* and septin 11 (*Sept11*), are also well represented in the over-expressed genes of the P1 knockouts.

Map kinase 8 (Mapk8) (also known as JNK1) is part of the Agtr1 signaling cascade and is one of the most significantly up-regulated genes in the P1 knockout brains. It has been shown to be a regulator of morphogenesis in early nervous system development [24]. JNK1 phosphorylates the microtubule depolymerizing factor SCG10 which determines microtubule stability and axodendritic length [24].

The up-regulation of conserved helix-loop-helix ubiquitous kinase (*Chuk*) (also known as IKK1) in the P1 brains is significant in that it is also influenced by angiotensin II [25], and activates the NF-kappa-B complex, which in turn causes cell proliferation and anti-apoptotic effects [26]. Notch gene homolog 2 (*Notch2)* and *Htt* are up-regulated in P1 knockouts and both have anti-apoptotic effects [27–29]. *Htt* up-regulates brain derived neurotrophic factor (BDNF) [30] and associates with the epidermal growth factor (EGF) pathway, potentially causing over-growth of neuronal cells. Notch2 is also negatively associated with glial differentiation [31].

Consistent with previous findings that Agtr2 induces apoptosis, three genes down-regulated in E15 *Agtr2*$^{-/y}$ brains, *Ptges2*, histocompatibility 2, T region locus 10 (*H2-T10*) and *Ube2m*, are all involved in inducing apoptosis.

In the P1 knockouts several over-expressed genes, AMPA-selective glutamate receptor 4 (*Gria4*), glutaminase (*Gls*) and *Htt*, were found to be involved in glutamate metabolism. Glutamate metabolism is integral to NMDA receptors which are essential in neuronal development and synaptic plasticity.

Other important up-regulated genes in the P1 list are the cell adhesion genes (*Ncam1, Gria4*, nuclear receptor subfamily 1, group I, member 3 (*Nr1i3*) and *Mapk8*). *Ncam1*, neural cell adhesion molecule 1, has been associated with NMDA receptors [32] and the inhibition of cell death [33]. Poliovirus receptor-related 4 (*Pvrl4*) is also a cell to cell adhesion gene [34]. *Ncam1, Gria4, Nr1i3* and *Mapk8* all share several important neurological functions (Fig. 2B).

Discussion

Cognitive function and adaptive behavior are two major functions of the brain that are consistently found to be impaired at variable levels in people with intellectual disability. Several genes, when defective, have been identified that cause learning and memory impairment in humans and mice. A role for *Agtr2* in brain development and function has been suggested and a likely involvement of *AGTR2* in human ID has been previously shown [2–6]. A detailed examination in *Agtr2*-deficient mice further revealed a deficit in spatial memory that was not related to fear [7,8]. These mice have demonstrated cellular over-growth in all examined brain regions [35]. Importantly, these mice showed abnormal dendritic spine morphology and length [9]. Both features are also found in some cases of ID. Thus, these mice provided a model system for studying genes whose function might be dependent or influenced by *Agtr2* gene function.

Expression of Agtr2 has been shown to be variable and transient in various brain structures during embryogenesis with expression declining rapidly after birth [13,22]. We confirmed expression of the *Agtr2* gene at the E15 stage of mouse embryonic brain and chose to use this developmental stage to study the impact of *Agtr2* gene action. We examined expression levels of 44,000 probes representing approximately 25,000 genes in *Agtr2* $^{-/y}$ and control mouse brains at developmental stage E15 and at birth (P1). Significant differences in gene expression were demonstrated by hierarchical clustering and *t-test* analyses. *Agtr2*$^{-/y}$ samples grouped together and were distinct from control samples.

Expression profiles of *Agtr2*$^{-/y}$ brains also shed light on possible cellular mechanisms and genes that might be contributing to the cognitive impairment and defective dendritic morphology observed in these mice [9]. These mice had altered spine morphology in areas of CA1, including stubby, enlarged spine formation, aberrant protrusions, and hydropic spine degeneration [9]. Dendritic spines and their morphological plasticity play a critical role in learning and memory function of the brain. Many forms of ID have been shown to be associated with abnormalities in dendritic spine morphology and structure [10–12,36]. The structure and dynamics of these structures have been shown to be influenced by the underlying actin-cytoskelton and microtubules. Thus the expression levels of genes regulating these structures are likely to play a critical role. Similar findings were previously reported in Fmr-1 knockout mice [12]. Interestingly, several genes up-regulated in *Agtr2*$^{-/y}$ brains are involved in cytoskeleton and microtubule regulation. The over-expression of these genes may potentially lead to alterations in the actin-cytoskeleton and dendritic spine seen in *Agtr2*$^{-/y}$ mouse brains.

Several genes involved in apoptosis were down regulated in E15 *Agtr2*$^{-/y}$ brains which support a role for Agtr2 as a mediator of apoptosis. Consistently, genes involved in anti-apoptosis activities were upregulated in P1 *Agtr2*$^{-/y}$ brains and may reflect the increase in the number of neuronal cells observed in adult *Agtr2*$^{-/y}$ mice brain regions [35].

Surprisingly only two dysregulated genes, *Pisd* and *Rab30*, were found in common between the two developmental stages. Significance of this observation is not clear. However, differences in expression of Agtr2 influenced genes at two different time points of brain development may relate to the observed variation in *Agtr2* gene expression during embryogenesis [13,22].

Activation of Agtr2 has been shown to negatively regulate some of the actions of Agtr1 [37]. The absence of Agtr2 did not cause increased expression of Agtr1 in the brains of E15 or P1 *Agtr2*$^{-/y}$ mice. There was also no difference in the expression of several genes in the RAS between knockouts and controls (data not shown). However, our results show that genes downstream of *Agtr1* are up-regulated in the absence of *Agtr2*.

Previous studies have indicated involvement of Agtr2 in various signaling cascades influencing neurite outgrowth and elongation, neuronal differentiation, cell proliferation, growth inhibition and induction of apoptosis [20,38–41]. Furthermore, Agtr2 has also been shown to directly interact with a variety of proteins, ERBB3, ZBTB16, SLC9A6/NHE6 and MTUS1 [15–18]. Thus it is not surprising that our study revealed a great variety of Agtr2 influenced genes. However, a detailed mechanism of Agtr2 actions remains to be elucidated and it is conceivable that some of the Agtr2 effects are likely direct and others may be indirect.

The data in this study provide a first glimpse of the gene expression profile of developing and newborn brains in the absence of *Agtr2* expression. Although it would be premature to propose a direct link between genes dysregulated in *Agtr2*$^{-/y}$ brain and observed features in *Agtr2*$^{-/y}$ mice, the data provide clues to these functional correlations and can be examined

further by additional experimental means. Expression profiling using specific brain regions or at additional developmental stages may reveal critical genes that may have been masked in our analyses of whole brain. Further studies may reveal that dysregulation of expression of some of the genes influenced by Agtr2 may contribute either directly or through other factors to the pathophysiology of intellectual disability.

Materials and methods

Animals

Agtr2$^{-/y}$ mice were described previously [3,9] and are from the 129/sv strain on a C57BL/6 × 129 mixed genetic background with a disrupted *Agtr2* gene. Pre-dissected organs from *Agtr2*$^{-/y}$ and control mice were isolated from the breeding stocks maintained at the Charité, Campus Benjamin Franklin, Berlin, Germany. Experiments were conducted according to the guidelines of the National Act on Use of Experimental Animals of the German Federal State [9].

Animal genotyping was performed after isolating liver DNA using the Qiagen DNA tissue kit (Qiagen Inc., Valencia, CA) according to manufacturer's recommendation and was used for animal genotyping. PCR was performed with the following primer sets: knockout-NeoPvu-F, 5′-GGCAGCGCGGCTATCGTGG-3′ and control AT25-F, 5′-CCACCAGCAGAAACATTACC-3′ and the same reverse primer was used for both: AT23-R, 5′-GAACTACATAAGATGCTTGCCAGG-3′. The cycling conditions were: 95 ºC for 5 min followed by 30 cycles of 95 ºC for 30 sec, 60 ºC for 30 sec and 72 ºC for 45 sec, with a final extension of 7 min. Sex was determined by genotyping with an X-linked gene *Jarid1 C*, using the following primers: Forward, 5′-CTGAAGCTTTTGGCTTTGAG-3′ and reverse, 5′-CCACTGCCAAATTCTTTGG-3′ with the following conditions: initial denaturation at 95 °C for 5 min, followed by 20 sec at 95 °C, 30 sec at 56 °C, and 40 sec at 72 °C for 30 cycles with a final extension at 72 °C for 7 min [42]. *Jarid1 C* primers produced a 331 bp (chromosome X-specific fragment) and 302 bp (specific to a homologue to *Jarid1 C* on the Y chromosome) DNA fragments in males and a single 331 bp DNA fragment in females.

RNA extraction, cDNA synthesis and array hybridization

Total RNA was extracted from frozen whole brain samples weighing less than 30μg using the Qiagen RNeasy kit (Qiagen Inc., Valencia, CA) according to manufacturer instructions. Samples were cleaned with DNase using the Ambion Turbo DNase-free kit (Ambion Inc., Austin, TX). RNA samples were analyzed on the Agilent 2100 expert bioanalyzer (Agilent, Santa Clara, CA) for purity and concentration.

RNA from six male controls and eight male knockouts at stage E15 were amplified individually and labeled with the Agilent low RNA Input Linear Amplification Kit (Agilent, Santa Clara, CA) according to the manufacturer's instructions. In brief, cDNA was synthesized using a T7 primer and was then labeled with Cy3- or Cy5-CTP. Samples were purified with Qiagen RNasey mini spin columns (Qiagen, Valencia, CA). Equal amounts of control sample and *Agtr2*$^{-/y}$ sample were labeled with Cy3 or Cy5 respectively and were hybridized to the first set of 8 Agilent Whole Mouse Genome Oligo 44K Microarrays slides (Agilent, Santa Clara, CA) according to the manufacturer's protocol. On the second set of microarray slides, the control samples were paired with a different knockout sample. Arrays were hybridized for 17 hours at 65ºC and then washed with 6X SSC, 0.005% Triton X-102 for one min and then with 0.1X SSC, 0.005% Triton X-102 for one min and then for 30 sec in ozone scavenging solution (Agilent #5185–5979). The microarray slides were scanned on an Agilent microarray scanner and data was normalized and extracted with Feature

Extraction 8.0 software (Agilent, Santa Clara, CA). RNA from four male control and four P1 *Agtr2* $^{-/y}$ brains was handled in the same fashion, with all controls being dye-swapped with a different knockout in each dye selection.

Microarray analysis

MIAME-compliant microarray data files are located on the GEO site at http://www.ncbi.nlm.nih.gov/geo/query/acc.cgi?token=jnwbzucukeckkbs&acc=GSE12412 (project accession # GSE12412). Two arrays from the E15 set were not included due to poor hybridization. The data sets were first filtered for probes that had a presence in at least 50 percent of the arrays using dye swap as a parameter. This left 33,583 probes in the E15 data set and 32,974 probes in the P1 data set. Both data sets were then filtered by an absolute fold change of 2 fold (log10) or greater between knockouts and controls as determined by GeneSpring GX (Agilent, Santa Clara, CA). This filtering produced a list of 313 probes in the E15 set and 1340 probes in the P1 set. This data was then subject to a Student's t-test with a p-value ≤ 0.005 (which compared favorably to a similar test with a Benjamini and Hochberg False-Discovery rate of ≤ 0.01). This analysis led to an E15 list of 133 probes and a P1 list of 397 probes. Fold change (log2) was then calculated using limma [43,44]. The lists were further narrowed by using the most significant probes by fold change as determined by limma to a list of 62 transcripts for the E15 set and a similar number of transcripts for the P1 stage. Fold change (log2) threshold values of 1.3 and 1.4 as determined by limma were chosen for the E15 and P1 list respectively to generate a more focused set of genes for further analysis.

Hierarchical clustering (condition tree and gene tree) of the E15 and P1 arrays was performed by GeneSpring GX using a Pearson correlation with a clustering algorithm = average linkage, with a separation ratio of 1 and a minimum distance of 0.001 using the E15 or P1 final list.

Quantitative RT-PCR

RNA was isolated as previously described on four controls and four knockouts from each developmental stage, and from animals not used in the microarray experiment previously. Primers were designed using the Primer3 program (http://frodo.wi.mit.edu/cgi-bin/primer3/primer3_www.cgi) [45]. Biorad I-Script 1 step RT-PCR with SYBR green (Biorad, Hercules, CA) was used according to manufacturer instructions with 5 ng of RNA per sample used. Samples were run in triplicate on a Biorad i-cycler and analyzed using a standard curve method [46] and normalized to a control gene. The control gene, AK029535 (Riken cDNA493050c13) was selected from a list of genes showing the least difference in expression generated by limma using the model 1a algorithm as described earlier [47]. The list of primers used is in Supplementary Table 3. After normalization to the control gene, the mean log2 expression ratio for knockouts was divided by the same for controls, to arrive at the fold change. Two-tailed t-tests were implemented to determine significance of changes between the two groups.

Functional grouping, annotation and pathway analysis

Annotation of genes in the list was enhanced by using the DAVID Gene Id Conversion Tool with a p-value threshold of ≤ 0.05 [48]. Gene ontology for genes in the final lists was also enhanced individually investigating the gene ontology information provided by the Entrez Gene search tool of NCBI.

Pathway Studio (Ariadne Genomics, Rockville, MD) was utilized by loading each up or down-regulated list and using the shortest path function. This software builds a network from information available from curated databases. This information is used to draw

functional relationships between proteins, cell objects, small molecules, diseases and cell processes.

Supplementary Material

Refer to Web version on PubMed Central for supplementary material.

Acknowledgments

We thank Drs. Liangjiang Wang and Julianne Collins for helpful discussions and technical assistance. We also thank Dr Minoru Ko for assistance in experimental planning. This work was supported, in part, by a grant from the NIH (R01 HD39331) to A.K.S. and a grant from the South Carolina Department of Disabilities and Special Needs (SCDDSN).

References

1. Inlow JK, Restifo LL. Molecular and comparative genetics of mental retardation. Genetics. 2004; 166:835–881. [PubMed: 15020472]
2. Hein L, Barsh G, Pratt R, Dzau V, Kobilka B. Behavioral and cardiovascular effects of disrupting the angiotensin II type-2 receptor gene in mice. Nature. 1995; 377:744–747. [PubMed: 7477266]
3. Ichiki T, et al. Effects on blood pressure and exploratory behavior of mice lacking angiotensin II type-2 receptor. Nature. 1995; 377:748–750. [PubMed: 7477267]
4. Vervoort VS, et al. AGTR2 mutations in X-linked mental retardation. Science. 2002; 296:2401–2403. [PubMed: 12089445]
5. Bienvenu T, et al. Rare polymorphic variants of the AGTR2 gene in boys with non-specific mental retardation. J Med Genet. 2003; 40:357–359. [PubMed: 12746399]
6. Ylisaukko-ojo T, et al. Identification of two AGTR2 mutations in male patients with non-syndromic mental retardation. Hum Genet. 2004; 114:211–213. [PubMed: 14598163]
7. Okuyama S, Sakagawa T, Chaki S, Imagawa Y, Ichiki T, Inagami T. Anxiety-like behavior in mice lacking the angiotensin II type-2 receptor. Brain Res. 1999; 821:150–159. [PubMed: 10064799]
8. Sakagawa T, et al. Pain threshold, learning and formation of brain edema in mice lacking the angiotensin II type 2 receptor. Life Sci. 2000; 67:2577–2585. [PubMed: 11104359]
9. Maul B, et al. Impaired spatial memory and altered dendritic spine morphology in angiotensin II type 2 receptor-deficient mice. J Mol Med. 2008; 86:563–571. [PubMed: 18335189]
10. Grossman AW, Elisseou NM, McKinney BC, Greenough WT. Hippocampal pyramidal cells in adult Fmr1 knockout mice exhibit an immature-appearing profile of dendritic spines. Brain Res. 2006; 1084:158–164. [PubMed: 16574084]
11. Irwin SA, Galvez R, Greenough WT. Dendritic spine structural anomalies in fragile-X mental retardation syndrome. Cereb, Cortex. 2000; 10:1038–1044. [PubMed: 11007554]
12. Irwin SA, et al. Abnormal dendritic spine characteristics in the temporal and visual cortices of patients with fragile-X syndrome: a quantitative examination. Am J Med Genet. 2001; 98:161–167. [PubMed: 11223852]
13. Grady EF, Sechi LA, Griffin CA, Schambelan M, Kalinyak JE. Expression of AT2 receptors in the developing rat fetus. J Clin Invest. 1991; 88:921–933. [PubMed: 1885777]
14. Gendron L, Payet MD, Gallo-Payet N. The angiotensin type 2 receptor of angiotensin II and neuronal differentiation: from observations to mechanisms. J Mol Endocrinol. 2003; 31:359–372. [PubMed: 14664700]
15. Knowle D, Ahmed S, Pulakat L. Identification of an interaction between the angiotensin II receptor sub-type AT2 and the Erb3 receptor, a member of the epidermal growth factor receptor family. Regulatory Peptides. 2000; 87:73–82. [PubMed: 10710290]
16. Nouet S, et al. Trans-inactivation of receptor tyrosine kinases by novel angiotensin II AT2 receptor-interacting protein. ATIP, J Biol Chem. 2004; 279:28989–28997.

17. Pulakat L, et al. Ligand-dependent complex formation between the Angiotensin II receptor subtype AT2 and Na+/H+ exchanger NHE6 in mammalian cells. Peptides. 2005; 26:863–873. [PubMed: 15808917]
18. Senbonmatsu T, et al. A novel angiotensin II type 2 receptor signaling pathway: possible role in cardiac hypertrophy. EMBO J. 2003; 22:6471–6482. [PubMed: 14657020]
19. Gilfillan GD, et al. SLC9A6 mutations cause X-linked mental retardation, microcephaly, epilepsy, and ataxia, a phenotype mimicking Angelman syndrome. Am J Hum Genet. 2008; 82:1003–1010. [PubMed: 18342287]
20. Stroth U, Meffert S, Gallinat S, Unger T. Angiotensin II and NGF differentially influence microtubule proteins in PC12W cells: role of the AT2 receptor. Mol Brain Res. 1998; 53:187–195. [PubMed: 9473667]
21. Bjorkblom B, et al. Constitutively active cytoplasmic c-Jun N-terminal kinase 1 is a dominant regulator of dendritic architecture: role of microtubule-associated protein 2 as an effector. J Neurosci. 2005; 25:6350–6361. [PubMed: 16000625]
22. Nuyt AM, Lenkei Z, Palkovits M, Corvol P, Llorens-Cortes C. Ontogeny of angiotensin II type 2 receptor mRNA expression in fetal and neonatal rat brain. J Comp Neurol. 1999; 407:193–206. [PubMed: 10213091]
23. Sun Y, Kaksonen M, Madden DT, Schekman R, Drubin DG. Interaction of Sla2p's ANTH domain with PtdIns(4,5)P2 is important for actin-dependent endocytic internalization. Mol Biol Cell. 2005; 16:717–730. [PubMed: 15574875]
24. Tararuk T, et al. JNK1 phosphorylation of SCG10 determines microtubule dynamics and axodendritic length. J Cell Biol. 2006; 173:265–277. [PubMed: 16618812]
25. Wu L, Iwai M, Li Z, Li JM, Mogi M, Horiuchi M. Nifedipine inhibited angiotensin II-induced monocyte chemoattractant protein 1 expression: involvement of inhibitor of nuclear factor kappa B kinase and nuclear factor kappa B-inducing kinase. J Hypertens. 2006; 24:123–130. [PubMed: 16331110]
26. Luo JL, Kamata H, Karin M. IKK/NF-kappaB signaling: balancing life and death--a new approach to cancer therapy. J Clin Invest. 2005; 115:2625–2632. [PubMed: 16200195]
27. Duechler M, Shehata M, Schwarzmeier JD, Hoelbl A, Hilgarth M, Hubmann R. Induction of apoptosis by proteasome inhibitors in B-CLL cells is associated with downregulation of CD23 and inactivation of Notch2. Leukemia. 2005; 19:260–267. [PubMed: 15565166]
28. Leavitt BR, et al. Wild-type huntingtin protects neurons from excitotoxicity. J Neurochem. 2006; 96:1121–1129. [PubMed: 16417581]
29. Rigamonti D, et al. Wild-type huntingtin protects from apoptosis upstream of caspase-3. J Neurosci. 2000; 20:3705–3713. [PubMed: 10804212]
30. Zuccato C, et al. Huntingtin interacts with REST/NRSF to modulate the transcription of NRSE-controlled neuronal genes. Nat Genet. 2003; 35:76–83. [PubMed: 12881722]
31. Tanaka M, Kadokawa Y, Hamada Y, Marunouchi T. Notch2 expression negatively correlates with glial differentiation in the postnatal mouse brain. J Neurobiol. 1999; 41:524–539. [PubMed: 10590176]
32. Sytnyk V, Leshchyns'ka I, Nikonenko AG, Schachner M. NCAM promotes assembly and activity-dependent remodeling of the postsynaptic signaling complex. J Cell Biol. 2006; 174:1071–1085. [PubMed: 17000882]
33. Bussolati B, et al. Neural-cell adhesion molecule (NCAM) expression by immature and tumor-derived endothelial cells favors cell organization into capillary-like structures. Exp Cell Res. 2006; 312:913–924. [PubMed: 16406048]
34. Reymond N, Fabre S, Lecocq E, Adelaide J, Dubreuil P, Lopez M. Nectin4/PRR4, a new afadin-associated member of the nectin family that trans-interacts with nectin1/PRR1 through V domain interaction. J Biol Chem. 2004; 276:43205–43215. [PubMed: 11544254]
35. von Bohlen und Halbach O, Walther T, Bader M, Albrecht D. Genetic deletion of angiotensin AT2 receptor leads to increased cell numbers in different brain structures of mice. Regul Pept. 2001; 99:209–216. [PubMed: 11384784]
36. Nadif Kasri N, Van Aelst L. Rho-linked genes and neurological disorders. Pflugers Arch. 2008; 455:787–797. [PubMed: 18004590]

37. AbdAlla S, Lother H, Abdel-tawab AM, Quitterer U. The angiotensin II AT2 receptor is an AT1 receptor antagonist. J Biol Chem. 2001; 276:39721–39726. [PubMed: 11507095]
38. Beaudry H, Gendron L, Guimond MO, Payet MD, Gallo-Payet N. Involvement of protein kinase C alpha (PKC alpha) in the early action of angiotensin II type 2 (AT2) effects on neurite outgrowth in NG108-15 cells: AT2-receptor inhibits PKC alpha and p21ras activity. Endocrinology. 2006; 147:4263–4272. [PubMed: 16740968]
39. Berry C, Touyz R, Dominiczak AF, Webb RC, Johns DG. Angiotensin receptors: signaling, vascular pathophysiology, and interactions with ceramide. Am J Physiol Heart Circ Physiol. 2001; 281:H2337–2365. [PubMed: 11709400]
40. Li JM, et al. Angiotensin II-Induced Neural Differentiation via Angiotensin II Type 2 (AT2) Receptor-MMS2 Cascade Involving Interaction between AT2 Receptor-Interacting Protein and Src Homology 2 Domain-Containing Protein-Tyrosine Phosphatase 1. Mol Endocrinol. 2007; 21:499–511. [PubMed: 17068200]
41. Meffert S, Stoll M, Steckelings UM, Bottari SP, Unger T. The angiotensin II AT2 receptor inhibits proliferation and promotes differentiation in PC12W cells. Mol Cell Endocrinol. 1996; 122:59–67. [PubMed: 8898348]
42. Clapcote J, Roder J. Simplex PCR assay for sex determination in mice. Biotechniques. 2005; 38:702–706. [PubMed: 15945368]
43. Yee H. marray: Exploratory analysis for two-color spotted microarray data. R package version 1.8.0. 2005
44. Smyth, G. Limma: linear models for microarray data. New York: Springer; 2005.
45. Rozen S, Skaletsky H. Primer3 on the WWW for general users and for biologist programmers. Methods Mol Biol. 2000; 132:365–386. [PubMed: 10547847]
46. Larionov A, Krause A, Miller W. A standard curve based method for relative real time PCR data processing. BMC Bioinformatics. 2005; 6:62. [PubMed: 15780134]
47. Szabo A, Perou CM, Karaca M, Perreard L, Quackenbush JF, Bernard PS. Statistical modeling for selecting housekeeper genes. Genome Biol. 2004; 5:R59. [PubMed: 15287981]
48. Dennis G Jr, Sherman BT, Hosack DA, Yang J, Gao W, Lane HC, Lempicki RA. DAVID: Database for Annotation, Visualization, and Integrated Discovery. Genome Biol. 2003; 4:P3. [PubMed: 12734009]

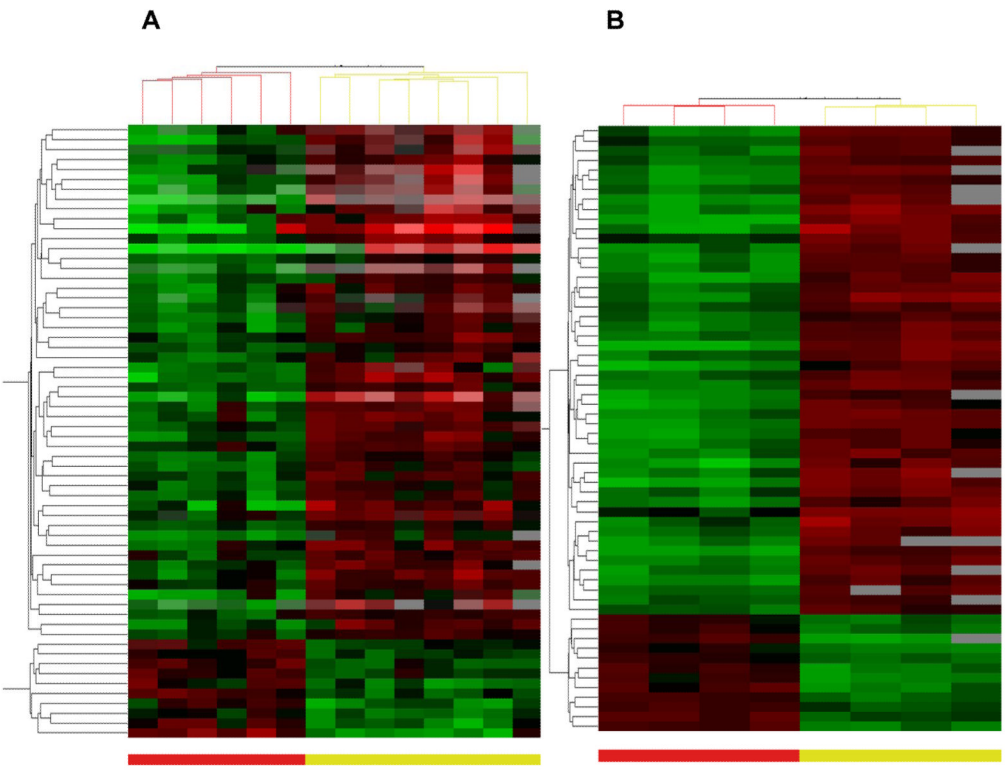

Fig. 1.

Hierarchical clustering showing knockout animals have different expression profiles as represented by the dye swap color coding below the tree, with the red bar and tree branches being the control group and yellow the *Agtr2*$^{-/y}$ group. Each row is a probe, each column is the array of an individual animal brain. Red represents up-regulation and green down-regulation. Gray represents lack of hybridization. (A) embryo (E15) arrays (B) postnatal day one (P1) arrays. Condition tree is on the top each heat map with each dye-set represented by a different color on the tree branches. A gene tree is on the left side of each heat map.

Fig. 2A

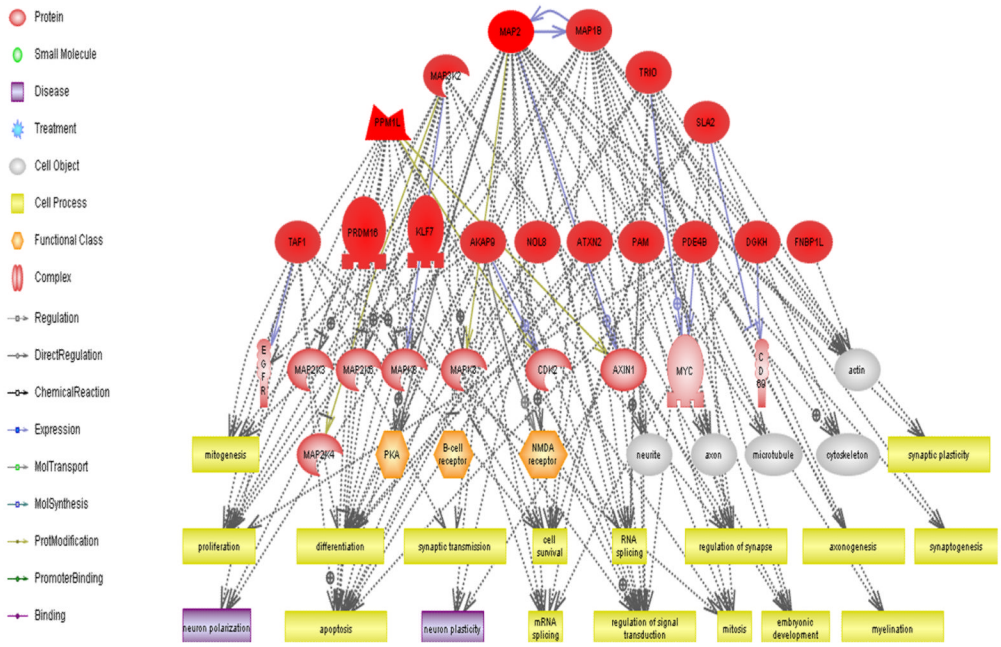

Fig. 2B

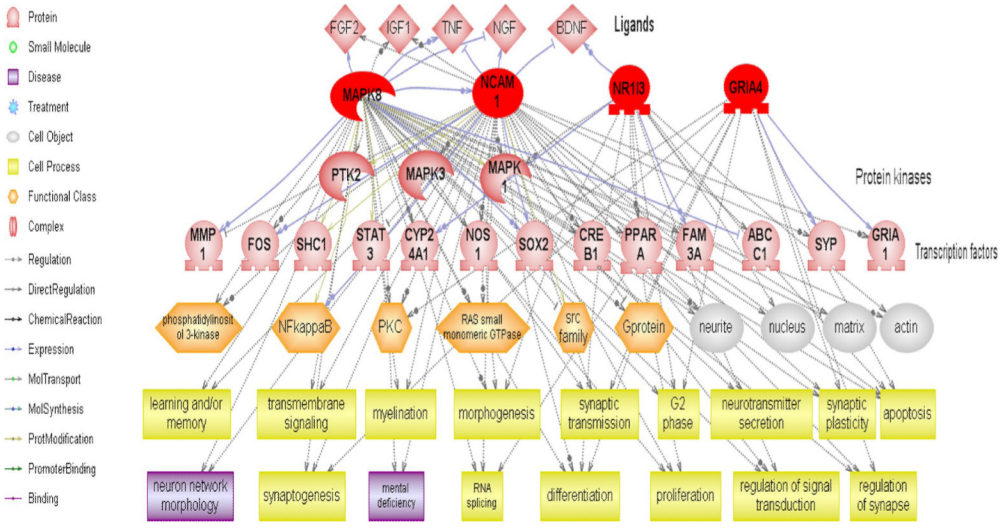

Fig. 2.

Pathway analysis of selected up-regulated transcripts in *Agtr2*$^{-/y}$ brains (A) Transcripts up-regulated in *Agtr2*$^{-/y}$ embryo brains are involved in pathways affecting microtubules, actin and cytoskeleton expression as well as other cell functions vital to brain development and

function. Genes highlighted in red are from the E15 list. (B) Genes with common neurological functions are up-regulated in P1 knockouts. Red shapes = genes from P1 list. Makp8, Ncam, Nri3 and Gria4 have interactions with many ligands, transcription factors and protein kinases in common. Down-stream effects of these up-regulated transcripts have many effects on neurological functions such as synaptic transmission and regulation as well as cell proliferation and differentiation.

Table 1

Genes at developmental stage E15 showing fold change ≥ 1.3 and $p < 0.005$ in Agtr2$^{-/y}$ brains

Probe set	Genebank	Gene Symbol	Gene Description	P value	Fold Change
A_51_P514139	NM_027504	Prdm16	PR domain containing 16	1.97E-04	+3.1
A_52_P546610	NM_013626	Pam	peptidylglycine alpha-amidating monooxygenase	6.72E-05	+2.1
A_51_P337944	**NM_080708**	**Bmp2k**	**BMP2 inducible kinase**	**7.96E-07**	**+1.9**
A_52_P561377	NM_145505	Fam160b1	family with sequence similarity 160, member B1	1.88E-05	+1.9
A_52_P542860	NM_172618	Btbd9	BTB (POZ) domain containing 9	1.61E-03	+1.8
A_52_P135424	AK032599			1.45E-03	+1.6
A_52_P654624	**AK005333**	**Pisd**	**phosphatidylserine decarboxylase**	**1.08E-04**	**+1.6**
A_52_P342836	BC055351	Hn1l	hematological and neurological expressed 1-like	2.83E-03	+1.6
A_52_P150396	AK013803	Akirin2	akirin 2	9.00E-05	+1.6
A_52_P54666	AK086484	Mtap2	microtubule-associated protein 2	4.68E-04	+1.6
A_52_P188425	BC047992;	Prosc	proline synthetase co-transcribed	5.66E-04	+1.5
A_51_P247114	NM_008199	H2-BL	histocompatibility 2, blastocyst	8.23E-06	+1.5
A_52_P617386	AK084084	Rab30	RAB30, member RAS oncogene family	6.86E-04	+1.5
A_51_P393161	AK049497	*Scaper*	S-phase cyclin A-associated protein in ER	1.33E-04	+1.5
A_51_P496779	NM_194462	Akap9	A kinase (PRKA) anchor protein (yotiao) 9	1.40E-04	+1.5
A_51_P446575	AK044903	Fnbp1l	formin binding protein 1-like	2.56E-04	+1.4
A_52_P207132	AK044972	Plcxd3	phosphatidylinositol-specific phospholipase C, X domain containing 3	5.10E-04	+1.4
A_52_P462472	XM_205178	C77370	expressed sequence C77370	9.91E-05	+1.4
A_52_P110581	AK050558	A930011G23Rik	RIKEN cDNA A930011G23 gene	1.13E-04	+1.4
A_51_P212515	NM_178726	Ppm1l	protein phosphatase 1 (formerly 2C)-like	1.55E-03	+1.4
A_51_P227866	AK030696	Tmx4	Thioredoxin-related transmembrane protein 4	2.31E-04	+1.4
A_52_P503135	NM_177054	Casc4*	cancer susceptibility candidate 4	1.47E-03	+1.4
A_52_P90101	AK036209	Atxn2	ataxin 2	1.85E-03	+1.4
A_51_P172241	TC1312974			4.07E-05	+1.4
A_52_P660753	XM_194622	Taf1	TATA box binding protein (TBP)-associated factor	8.54E-04	+1.4
A_52_P239424	AK086122	Klf7*	Kruppel-like factor 7	8.96E-04	+1.4

Probe set	Genebank	Gene Symbol	Gene Description	P value	Fold Change
A_52_P424197	AK029131	Map3k2	mitogen-activated protein kinase kinase kinase 2	4.43E-04	+1.4
A_51_P366277	BC049166	Nol8	nucleolar protein 8	1.14E-03	+1.4
A_52_P16346	AK012005;	Sla2	Src-like-adaptor 2	1.93E-04	+1.4
A_52_P268720	BC021818	Helz	helicase with zinc finger domain	2.30E-04	+1.4
A_51_P134801	XM_619483	Ankrd12	ankyrin repeat domain 12	2.95E-04	+1.4
A_51_P308628	XM_619630	Nbeal1	neurobeachin like 1	1.07E-03	+1.4
A_51_P128075	NM_027028	1700008P20Rik	RIKEN cDNA 1700008P20 gene	1.16E-03	+1.4
A_52_P407755	**AK009137**	**Prei4**	**preimplantation protein 4**	**1.14E-03**	**+1.4**
A_51_P512340	NM_019840	Pde4b	phosphodiesterase 4B, cAMP specific	1.35E-04	+1.3
A_51_P364894	NM_054089	Tgs1	Trimethylguanosine synthase homolog (S. cerevisiae)	2.90E-03	+1.3
A_52_P462171	XM_354675	Arid4a	AT rich interactive domain 4A (RBP1-like)	6.96E-04	+1.3
A_51_P217878	AK043468	Mtap1b	microtubule-associated protein 1B	3.78E-04	+1.3
A_52_P167166	AK047842	Shprh	SNF2 histone linker PHD RING helicase	4.26E-04	+1.3
A_52_P540045	AK083897	Dgkh	diacylglycerol kinase, eta	1.39E-03	+1.3
A_52_P289071	NM_177054	Casc4*	cancer susceptibility candidate 4	5.10E-04	+1.3
A_51_P115940	NM_172787	L3mbtl3	l(3)mbt-like 3 (Drosophila)	3.44E-04	+1.3
A_52_P5549	NM_026583	5830415L20Rik	RIKEN cDNA 5830415L20 gene	1.11E-04	+1.3
A_52_P38317	AK046153	Nat5	N-acetyltransferase 5 (ARD1 homolog, S. cerevisiae)	1.36E-03	+1.3
A_51_P127215	BC003348	Sesn3	sestrin 3	3.77E-03	+1.3
A_51_P405280	NM_033563	Klf7*	Kruppel-like factor 7 (ubiquitous)	5.19E-04	+1.3
A_52_P190807	AK032690	Fam92a	family with sequence similarity 92, member A	9.75E-04	+1.3
A_52_P519538	NM_172712	Uba6	ubiquitin-like modifier activating enzyme 6	1.11E-04	+1.3
A_52_P197199	XM_139187	Pcdh9	protocadherin 9	2.01E-04	+1.3
A_52_P521507	BC051169	Trio	triple functional domain (PTPRF interacting)	5.54E-04	+1.3
A_52_P621817	AK173240	Zfp46	zinc finger protein 46	2.49E-04	+1.3
A_52_P651784	XM_486486	discontinued record		1.15E-04	+1.3
A_51_P349008	NM_133783	Ptges2	prostaglandin E synthase 2	3.86E-04	−1.3
A_51_P218805	NM_212443	Gfer	growth factor, erv1 (S. cerevisiae)-like (augmenter of liver regeneration)	9.44E-04	−1.3
A_52_P108808	TC1316888			5.85E-04	−1.3

Probe set	Genebank	Gene Symbol	Gene Description	P value	Fold Change
A_52_P20639	NM_023727	Rd3	retinal degeneration 3	2.41E-04	−1.3
A_51_P506937	NM_011885	Mrps12	mitochondrial ribosomal protein S12	5.48E-04	−1.3
A_51_P432538	NM_010395	H2-t10	histocompatibility 2, T region locus 10	5.17E-04	−1.3
A_51_P344566	NM_011121	Plk1	polo-like kinase 1	2.81E-05	−1.4
A_51_P272172	NM_053068	Chrac1	chromatin accessibility complex 1	3.74E-04	−1.4
A_51_P100246	**NM_145578**	**Ube2m**	**ubiquitin-conjugating enzyme E2M (UBC12 homolog, yeast)**	**1.00E-03**	**−1.4**
A_51_P288549	BC016255	Pla2g4b	phospholipase A2, group IVB (cytosolic)	1.54E-05	−1.7

*Genes listed twice with two separate probes: NM_177054 (Casc4) and NM_033563 (Klf7); Relative expression of genes highlighted in bold types is also checked by quantitative RT-PCR.

Table 2

Genes at P1 Showing Fold Change ≥ 1.4 and $p < 0.005$ in $Agtr2^{-/y}$ Brains

Probe Set	Genebank	Gene Symbol	Gene Description	P Value	Fold Change
A_51_P222953	AK047664	Gls	Glutaminase	8.890E-06	+2.2
A_52_P329105	NM_134077	Rbm26	RNA binding motif protein 26	4.510E-03	+2.1
A_52_P386075	XM_622182	LOC623078		1.040E-03	+2.1
A_51_P304449	**AK031960**	**Add1**	**adducin 1 (alpha)**	**1.270E-04**	**+2.0**
A_51_P390755	AK035845	Ptprs	protein tyrosine phosphatase, receptor type, S	1.380E-04	+2.0
A_52_P654624	**AK005333**	**Pisd**	**phosphatidylserine decarboxylase**	**3.390E-04**	**+1.9**
A_52_P657817	AK030767	Mapk8	mitogen-activated protein kinase 8	5.090E-04	+1.9
A_52_P368881	TC1323355			3.770E-04	+1.9
A_52_P102630	AB063319	Rian	RNA imprinted and accumulated in nucleus	4.280E-04	+1.8
A_52_P320822	NM_009186	Tra2b	Transformer 2 beta homolog (Drosophila)	7.950E-04	+1.8
A_52_P236097	AK017529	Sf3b3	splicing factor 3b, subunit 3	7.340E-04	+1.8
A_52_P92213	AK089867	2210404J11Rik	RIKEN cDNA 2210404J11 gene	8.570E-04	+1.7
A_52_P386468	**NM_007700**	**Chuk**	**conserved helix-loop-helix ubiquitous kinase**	**2.200E-06**	**+1.7**
A_52_P475033	AK088515	Usp15	ubiquitin specific peptidase 15	9.930E-04	+1.7
A_52_P617386	AK084084	Rab30	RAB30, member RAS oncogene family	1.220E-04	+1.7
A_52_P422088	AK084846	Ptbp2	polypyrimidine tract binding protein 2	5.190E-04	+1.7
A_52_P440027	AK014565	4632411B12Rik	RIKEN cDNA 4632411B12 gene	9.200E-04	+1.6
A_52_P24835	NM_027893	Pvrl4	poliovirus receptor-related 4	5.330E-04	+1.6
A_52_P484519	AK171368	Sept 11	septin 11	8.820E-04	+1.6
A_52_P319752	AK046219	Nudcd3	NudC domain containing 3	4.860E-04	+1.6
A_52_P527329	AK089867	2210404J11Rik	RIKEN cDNA 2210404J11 gene	8.570E-04	+1.6
A_51_P183154	AK049897	Hook1	hook homolog 1 (Drosophila)	6.280E-04	+1.6
A_52_P955951	AK048907	Gria4	glutamate receptor, ionotropic, AMPA4 (alpha 4)	2.170E-04	+1.6
A_52_P340618	BC030361	Eml5	echinoderm microtubule associated protein like 5	7.360E-04	+1.6
A_52_P323215	NM_019570	Rev 1	REV1 homolog (S. cerevisiae)	3.080E-05	+1.6
A_52_P433	AK129392	Saps3	SAPS domain family, member 3	5.040E-04	+1.6
A_52_P671465	**AK051363**	**Caprin 1**	**Cell cycle associated protein 1**	**2.720E-04**	**+1.6**

Probe Set	Genebank	Gene Symbol	Gene Description	P Value	Fold Change
A_51_P458230	AK054427			8.970E-04	+1.6
A_52_P276412	AK011886	Atpif1	ATPase inhibitory factor 1	6.450E-04	+1.6
A_52_P620432	AK019968	Fam82b	family with sequence similarity 82, member B	6.000E-04	+1.6
A_52_P398494	XM_902635	Ankrd11	ankyrin repeat domain 11	7.040E-04	+1.5
A_52_P113585	AK084575	Htt	Huntingtin	1.000E-04	+1.5
A_52_P411015	NM_177300	B130040O20Rik	RIKEN cDNA B130040O20 gene	6.150E-04	+1.5
A_52_P61903	AK014174	Chka	choline kinase alpha	4.240E-04	+1.5
A_52_P182520	BC028435	Timm9	translocase of inner mitochondrial membrane 9 homolog (yeast)	3.110E-04	+1.5
A_52_P668157	AK011905	Ncam1	neural cell adhesion molecule 1	8.800E-05	+1.5
A_52_P124105	AK083451	Rab14	RAB14, member RAS oncogene family	1.110E-04	+1.5
A_52_P98160	TC268598			5.940E-04	+1.5
A_52_P188026	BC051052	Ccar1	cell division cycle and apoptosis regulator 1	3.710E-04	+1.5
A_52_P59544	AK036220	Rbm18	RNA binding motif protein 18	3.110E-04	+1.5
A_52_P72938	AK039096	AI790442	expressed sequence AI790442	8.760E-04	+1.5
A_52_P321318	AF093677	mt-Atp6	ATP synthase 6, mitochondrial	3.140E-04	+1.5
A_52_P236607	BC066170	Ercc8	excision repaiross-complementing rodent repair deficiency, complementation group 8	3.100E-04	+1.4
A_52_P289213	BC059256	Notch2	Notch gene homolog 2 (Drosophila)	8.250E-04	+1.4
A_52_P454703	BE650851			3.580E-04	+1.4
A_51_P358256	NM_009803	Nr1i3	nuclear receptor subfamily 1, group I, member 3	6.810E-04	+1.4
A_52_P171993	AK012463	Psmd7	proteasome (prosome, macropain) 26S subunit, non-ATPase, 7	7.320E-04	+1.4
A_52_P146848	NM_016690	Hnrpdl	heterogeneous nuclear ribonucleoprotein D-like	2.740E-04	+1.4
A_52_P237755	TC1517524			8.580E-04	+1.4
A_52_P860487	ac1158020			6.740E-04	+1.4
A_51_P122246	NM_029720	Creld2	cysteine-rich with EGF-like domains 2	3.360E-04	−1.4
A_51_P281255	NM_016777	Nasp	nuclear autoantigenic sperm protein (histone-binding)	1.840E-04	−1.4
A_52_P576863	NM_025922	Itpa	inosine triphosphatase (nucleoside triphosphate pyrophosphatase)	8.830E-04	−1.4
A_51_P259001	NM_029814	Chmp5	chromatin modifying protein 5	3.150E-04	−1.4
A_52_P476357	NM_016878	Dnpep	aspartyl aminopeptidase	8.290E-04	−1.4
A_52_P141786	NM_029561	Ndfip2	Nedd4 family interacting protein 2	3.940E-04	−1.4

Probe Set	Genebank	Gene Symbol	Gene Description	P Value	Fold Change
A_51_P349142	NM_007991	Fbl	Fibrillarin	1.640E-04	−1.4
A_51_P479802	XM_110248	Fbxo11	F-box protein 11	2.630E-05	−1.4
A_51_P125535	**NM_017374**	**Ppp2cb**	**protein phosphatase 2 (formerly 2A), catalytic subunit, beta isoform**	**5.120E-04**	**−1.6**
A_51_P132978	NM_010497	Idh1	isocitrate dehydrogenase 1 (NADP+), soluble	7.520E-04	−1.6
A_51_P117226	AK046533	Zdhhc2	zinc finger, DHHC domain containing 2	1.020E-04	−1.6
A_51_P267544	**NM_013522**	**Frg1**	**FSHD region gene 1**	**6.180E-04**	**−1.6**

Relative expression of genes highlighted in bold types is also checked by quantitative RT-PCR.

Table 3

Q-RT-PCR Results of Selected Genes at E15 and Postnatal Day 1

Probe ID	Primary Accession	Gene	Dev. Stage	Fold Change	RT-PCR Fold Change	RT-PCR p-value
a_51_P337944	NM_080708	Bmp2k	E15	1.9	1.4	0.18
a_52_P654624	AK005333	Pisd	E15	1.6	2.3	0.05
a_52_P407755	AK009137	Prei4	E15	1.4	1.7	0.26
a_51_P488673 a_52_P404108	NM_008143	* Gnb2l1	E15	−1.3 −1.2	−1.5	0.09
a_51_P473533	L32836	* Ahcy	E15	−1.2	−1.7	0.01
a_51_P100246	NM_145578	Ube2m	E15	−1.4	−1.2	0.22
a_52_P654624	AK005333	Pisd	P1	1.9	1.7	0.02
a_52_P386468	NM_007700	Chuk	P1	1.7	1.4	0.05
a_51_P304449	AK031960	Add1	P1	2.0	1.7	0.10
a_52_P671465	AK051363	Caprin 1	P1	1.6	1.7	0.10
a_51_P125535	NM_017374	Ppp2cb	P1	−1.6	−1.4	0.07
a_51_P267544	NM_013522	Frg1	P1	−1.6	−1.7	0.08

* Genes with fold change ≤ −1.3 and thus are not included in Table 1.

Genomics. Author manuscript; available in PMC 2011 August 31.